# FACIAL PORE DETECTION BASED ON CHARACTERISTICS OF SKIN PIGMENT DISTRIBUTION

*Zhen Wang, Ruoxuan Li*

Department of Information Science and Technology, Tianjin University of Finance and Economics, China

## ABSTRACT

The facial pore feature is one of the crucial indicators for face recognition and skin evaluation. However, pores are tiny, which are difficult to detect and analysis based on the digital image. We proposed a new facial pore detection algorithm that combines the characteristics of skin pigment distribution and optimal scale, which can effectively eliminate the effect of complicated skin interferences from facial pore detection processing. First, considering the dissimilarity of skin pigment distribution on different pigment layers, we used SURF and SIFT algorithms to detect the skin features on different pigment layers and calculated the threshold by DBSCAN. Then, the Euclid distance was calculated to describe the positions similarity of the same detected points on different layers. Last, the optimal scales were set as thresholds to screen off the interferences of skin features except for pores. The experiment results confirm the improvement of the pore detection accuracy.

***Index Terms***— Facial pore detection, Skin pigment distribution, DBSCAN, Optimal scale

## 1. INTRODUCTION

Facial pore extraction and analysis are vitally crucial for data preparation for face characterization, and it is used for several applications such as skin evaluation, medical hairdressing, cosmetics development, face recognition, and facial reconstruction [1]. The recent methods of facial pore analysis process such as [2–4] need to use magnifying glasses, dermatoscope, spectrometers or macroscopic photography, which are of high cost and location limitations. Furthermore, pores can be used as a more unique and accurate feature for face recognition, facial reconstruction, and other fields. From a genetic point of view, the diverse elements that configure the skin are color, texture, pores, etc. They are formed from the embryo [5]. Therefore, it is believed that the number, structure, and measurement of each person's skin pores are unique relationships for everyone.

There are two kinds of pore detection methods to extract facial pores using digital images.

This work presented in the paper is partially supported by Natural Science Foundation of Tianjin (16JCYBJC42000).

The first kind is directly using original skin image. Malathi and Meena [6] proposed fingerprint pore detection using Scale-invariant feature transform(SIFT) [7], giving a new idea for facial pore detection. Li et al. [8, 9] proposed a facial pore detection and visualization method by using SIFT algorithm to made pore detection possible on digital images. However, this method is not effective at removing other facial interference features, such as moles, pockmarks, and the selected area for pore detection is limited to flat cheek area without reflection and shadow.

The second kind is using skin melanin layer image. As we know that the skin color, which is represented by a specific color space(RGB, CIELAB, etc.), is not an actual physical quantity but an abstract and derived human visual effect. And the color of the skin depends on the absorption and scattering of skin melanin and hemoglobin. Therefore, it is more authentic to study the skin features by obtaining the melanin and hemoglobin layer. Tsumura [10] split the average concentrations of melanin and hemoglobin by using Independent Components Analysis(ICA) over an RGB image, and reduced external disturbance on the skin such as shadows. Carlos [11] found that pores are mainly distributed on the melanin layer based on the absorption of light by different pigment layers. According to the research results of [12, 13], pores could be detected more accurately by using the separated melanin layer. However, the drawback of this kind of method is that some large facial features are not only composed of single pigment, such as acne marks and pigmented nevus. These significant features on the separated melanin layer will break into small features closed to pores, which will introduce new interference in facial pore detection. Therefore, it is still inaccurate to detect pores on the melanin layer, especially when we identify a large number of pores. In addition, similar with most facial pore detection methods, the facial pore analysis methods such as [14–16] are also need specific optical equipment, which are difficult for the dynamic, real-time, extensive applications.

Motivated by the above observations, in this paper we proposed a facial pore detection algorithm that combines the characteristics of skin pigment distribution and optimal scale. This algorithm can better deal with complicated skin interferences and improve the accuracy of pore detection by using multi-pigment skin images instead of single skin image.

## 2. FACIAL PORE DETECTION ALGORITHM

In order to overcome the shortcomings of existing pore detection methods, firstly, skin features are detected on different skin pigment layers obtained by using ICA method, Speeded-up robust features(SURF) [17] and SIFT algorithm. Then, Euclidean distance is introduced to describe the location similarity of skin features on different pigment layers, and the skin feature information on different pigmentation layers is linked together. Finally, the characteristics of skin pigment distribution and the optimal scale in SURF algorithm are used to set the boundary threshold, which can eliminate interferences from all skin features to pores. Algorithm 1 shows the facial pore detection algorithm clearly.

### 2.1. Skin Pigment Layers Separation

From an optics perspective, human skin is composed of different layers, which determines its optical properties and imaging model. The skin imaging process mainly consists of two processes: absorption and scattering. Two types of chromospheres cause absorption in the skin over the visible spectrum: melanin and hemoglobin; and scattering is caused by cells or cellular organelles [18]. When the incident light reaches the skin, part of the incident light is reflected on the surface of the skin, the rest penetrates into the skin layers. In the epidermal layer, the light is absorbed by melanin(minimal scattering), however, the light is scattered multiple times and absorbed by hemoglobin in the dermis layer. The absorption of light by melanin and hemoglobin largely determines the true appearance of the skin in color digital image. The pixel value of *R*, *G*, and *B* channels represents the amount of light whose reflected on the surface and entered the lens. Once lighting conditions changed, the facial skin features of the same person are different because of the shadows and reflections changing. Fortunately, this problem can be solved by obtaining stable true pigment layers such as melanin and hemoglobin.

Based on the Lambert-Beer Law [19], the equations of RGB value and pigment concentration can be constructed:

$$C_{B-R}^{log} = [v_m(R) - v_m(B)]\, c_m + [v_h(R) - v_h(B)]\, c_h + (\overline{E}_B^{log} - \overline{E}_R^{log})$$

$$C_{G-R}^{log} = [v_m(R) - v_m(G)]\, c_m + [v_h(R) - v_h(G)]\, c_h + (\overline{E}_G^{log} - \overline{E}_R^{log})$$

$$\begin{cases} C = \left[C_{B-R}^{log}, C_{G-R}^{log}\right]^T, \\ y = \begin{bmatrix} v_m(R) - v_m(B) & v_h(R) - v_h(B) \\ v_m(R) - v_m(G) & v_h(R) - v_h(G) \end{bmatrix} \\ \quad = [v_m, v_h], \\ c = [c_m, c_h]^T, \\ \overline{E} = \left[\overline{E}_B^{log} - \overline{E}_R^{log}, \overline{E}_G^{log} - \overline{E}_R^{log}\right]^T. \end{cases} \tag{1}$$

**Algorithm 1** Facial pore detection algorithm

**Input:** initial skin image; melanin layer image; hemoglobin layer image; $\omega_1$; $\omega_2$; $\omega_3$;

**Output:** Mark the pores on initial skin image by using $L_m^{'}$ ;

1: The location information of the detected points on melanin layer image $L_m = [x_m, y_m]$ was obtained by SIFT. The location information of the detected points on initial skin image $L_s = [x_s, y_s]$ and hemoglobin layer image $L_h = [x_h, y_h]$ were obtained by SURF. According to SURF algorithm, the optimal scale of interference detected on the initial skin image is obtained, as $S = (L_s; S_s)$.

2: Use the Euclidean distance $d_E(L_s, L_h)$ between $L_s$ and $L_h$ to screen off the interferences containing hemoglobin as well as maintain the interferences containing melanin. And $d_E(L_s, L_h) = \sqrt{(x_s - x_h)^2 + (y_s - y_h)^2}$, when $d_E(L_s(i), L_h(j) \le \xi \quad i, j = 1, 2, 3 \ldots$, the corresponding characteristics were deleted and $S$ was updated into $S^{'}$, $S^{'} = (L_s^{'}; S_s^{'})$, $L_s^{'} = \left[x_s^{'}, y_s^{'}\right]$. And $L_s(i) \in L_s$, $L_h(j) \in L_h$, $\xi$ expressed the maximum similarity of location information between the detection points on hemoglobin layer image and initial skin image. Because of the sizes of pores are less than one pixel, the range of $\xi$ is (0, 1).

3: Use the Euclidean distance $d_E(L_s^{'}, L_m)$ between $L_s^{'}$ and $L_m$ to screen off the interferences containing melanin and locate the pores accurately. And $d_E(L_s^{'}, L_m) = \sqrt{(x_s^{'} - x_m)^2 + (y_s^{'} - y_m)^2}$, when $d_E(L_s^{'}(p), L_m(q)) \le S_s^{'}(p) \quad p, q = 1, 2, 3 \ldots$, the corresponding characteristics were deleted and the location information of pores $L_m^{'}$ was obtained. And $L_s^{'}(p) \in L_s^{'}$, $S_s^{'}(p) \in S_s^{'}$, $L_m(q) \in L_m$, $S_s^{'}(p)$ were the optimal scales of the interferences containing melanin on $L_s^{'}(p)$.

The *V* is the linear combination of relative light absorbing vectors on melanin and hemoglobin layer, *E* represents minimum quantities associated with incident spectral radiation.The pigment densities *c* of melanin and hemoglobin are independent of each other, and *C* is linear combination of those two layers to represent difference among *R*, *G*, *B* channels. How to obtain the unknown pigment densities and its separation matrix is a Blind Source Separation(BBS) problem, and we can use ICA to solve it because the melanin and hemoglobin are mutually independent and non-gaussian. It is also worth noting that the formula establishes the relationship between the hypodermal reflex and the pigment densities.

### 2.2. Facial Pore Detection with Interferences Filter

After separating the layers of the melanin and hemoglobin pigment the realistic facial skin is acquired. However, the facial skin has not only the pores but also other skin features such as acne, redness and color spots. So we have to filter out these interferences for more accurate facial pores detection .

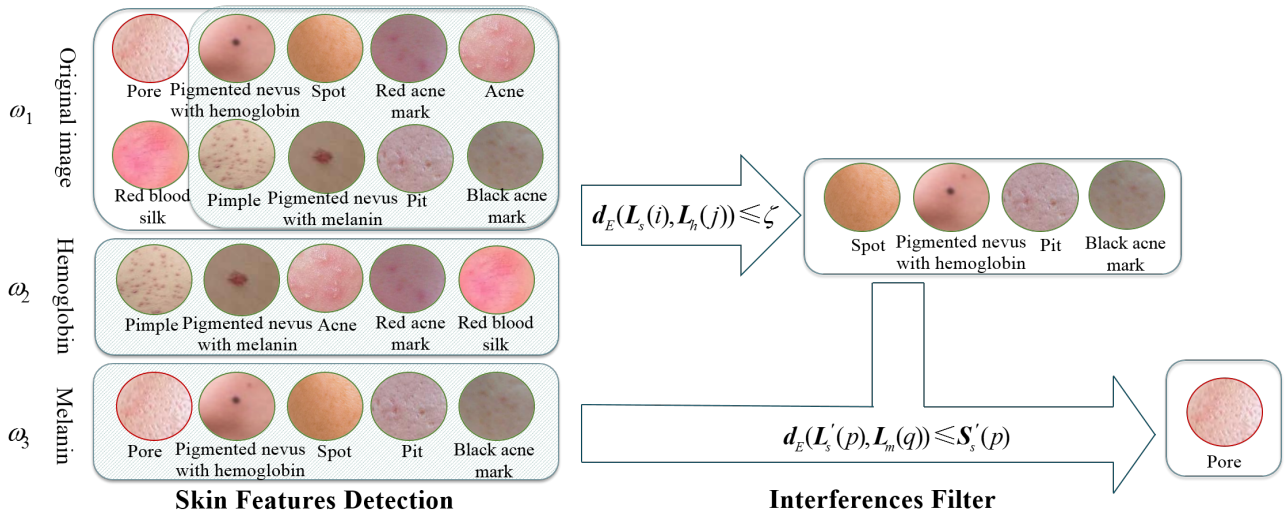


**Fig. 1**. Facial pore detection algorithm that eliminates interference.

Based on the analysis in [20], the size of facial pores varies in average is from 50um to 500um, which is far smaller than most of the other skin features on the initial skin image except for the redness. Redness is scattered, which causes its local saliency is close to facial pores. So it is difficult to use the initial image directly to distinguish redness and pores. Fortunately, redness only distributes on hemoglobin layer of the skin, when using the melanin layer to identify pores, redness can be effectively filtered out. However, there are also other facial skin features composed of melanin and hemoglobin on the melanin layer. In addition, during the separation of the pigment layers, significant skin features will be broken down into small features, which bring in new interferences for pore identification. It is difficult to detect the pores by using only one pigment layer, therefore, we take advantage of the difference of local saliency on different pigment layers to filter out interferences, and identify pores by using original skin image, melanin layer and hemoglobin layer together.

We classify the basic facial skin features into three layers according to distribution, as shown in Fig.1 left. Our facial pore detection algorithm combines the characteristics of skin pigment distribution and optimal scale, including skin features detection and interference screening as follows.

According to the difference of local salience between facial skin pores and other skin features, we identify pores and inferences by using SIFT and SURF algorithm, respectively. The SIFT is more accurately than SURF for detecting minor features. The SURF replaces the Gaussian second-order gradient template with box function to locate feature points, which is more efficiently. So for the sake of accuracy and efficiency of distinctive skin features detection, practically speaking, SIFT is used to detect all skin features including pores on melanin layer image, and SURF is used to detect all features including hemoglobin on hemoglobin layer and detect salient skin features on the original skin image. Because the salient skin features are considered as noise in pore detection. So we introduce Density-Based Spatial Clustering of Applications with Noise(DBSCAN) [21] to calculate a threshold for salient skin features classification based on Difference of Gaussian(DoG) responses in SURF. Algorithm 2 shows the threshold calculation process.

Based on the identification results of facial pores and interferences, the Euclidean distances between the detecting points on different skin layers are calculated. By using the characteristics of the skin pigment distribution we set flexible supremum threshold for the two kinds of similarities, between the interferences, and between the interferences and pores, to filter out interferences and preserve the pores. Firstly, in order to screen out the interferences with hemoglobin and retain the interferences with melanin in maximum, we set a minimum threshold for the Euclidean distance between the points on hemoglobin layer image and initial skin image. Then, Euclidean distance between the reserved interference with melanin and the detecting points on the melanin layer image is calculated, interferences containing melanin are filtered by choosing an optimal scale of distance. Here, we use the optimal scale in SURF to calculate the salient area with melanin as a flexible supremum threshold.

## 3. EXPERIMENTS

In this section, we evaluate the performances of our proposed facial pore detection algorithm. Because there is no standard data set of facial skin features at present, to facilitate comparative experiments, we choose the front face image in Bosphorus database [22] as the experimental image set. The area

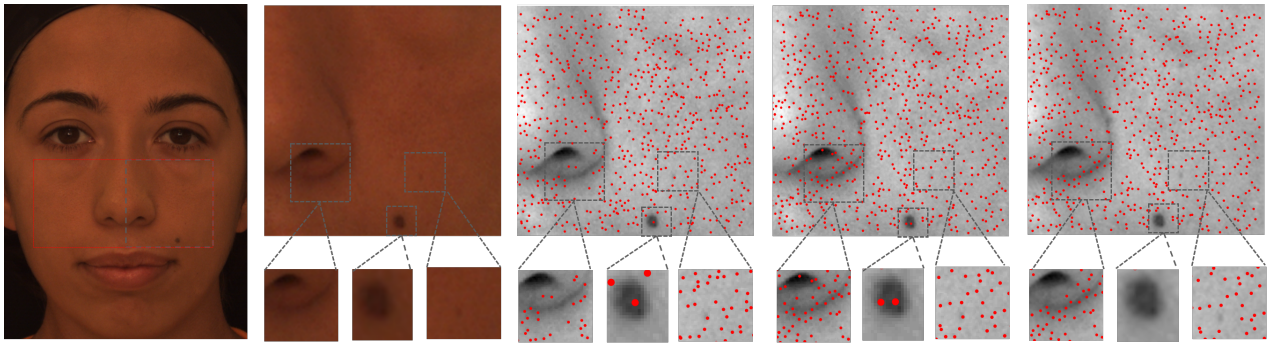


**Fig. 2**. Example of placing a figure with experimental results.

**Algorithm 2** Calculating the threshold using DBSCAN.

Detect the Dataset $S$ that is a set of the DoG responses for each initial skin image.
Record the number of skin image as $n$;
Determine the initial neighborhood radius $eps$;
Determine the minimum number of points required to form a cluster $MinPts$;
The fundamental vector is defined as $\boldsymbol{A}$;
Determine a small adjustment value as $\gamma$ ;
Determine the initial number of clusters as $m$.

**Input:** $S$; $eps$; $MinPts$; $n$; $\boldsymbol{A}$; $\gamma$;$m$;
**Output:** the threshold $\omega$ for features detection on initial skin images;

$m$=2
**while** ($m$>1) **do**
  **while** (the visited number i of $S_i$<n) **do**
    DBSCAN Algorithm to find the cluster representing pores.
    Record the number of clusters as m.
    Record the maximum $a_i$ in the cluster into $\boldsymbol{A}$.
  **end while**
  Compute the maximum of $\boldsymbol{A}$ as threshold $\omega$.
  $i$=0.
  $eps$=$eps$-$\gamma$.
**end while**

with the most concentrated facial pore was selected for comparative experiments such as the rectangle box in Fig.2(a), the height was from the highest lip point to the lowest eyelid point; the length was from left to right outer eye corner.

In order to verify the accuracy of facial pore detection and efficiency of screening out interferences, we compare the proposed method through the original skin image and skin melanin layer image. The filter rate of skin interferences $F$ defined as $F = 1 - I/M$ was used to evaluate the pore detection algorithm, where $I$ represents the number of detected interferences, and $M$ represents the number of labeled interferences. The interferences were labeled manually by 30 people with unanimous recognition. As shown in table 1, the filter rates for various interferences are significantly higher than the existing two pore detection algorithms, indicating efficiency of screening out other skin interferences. Fig.2 intuitively shows the result of facial pore detection. Compared with Fig.2(c), Fig.2(d) shows identified pores in shadow region thanks to the elimination of shadow influence, but neither of them can effectively eliminate the interference of other skin features. However, the proposed method can identify pores in shadow and effectively remove the interference of skin features such as pockmarks and pigmented moles, as shown in Fig.2(e), to identify pores more accurately.

**Table 1**. Filter rate $F\%$ of skin interferences

| Interferences | Original skin image | Melanin layer image | Proposed algorithm |
|---|---|---|---|
| Patch | 8.8929 | 5.3571 | 80.3571 |
| Pigmented nevus | 9.0909 | 36.3636 | 92.7273 |
| Papule /Acne | 7.6923 | 96.1538 | 96.1538 |
| Acne marks | 11.6279 | 53.4884 | 90.6977 |
| Pockmarks | 9.6774 | 16.1290 | 95.1613 |
| Redness | 14.2857 | 96.1905 | 98.0952 |
| Average | 9.9905 | 58.5163 | 92.1987 |

## 4. CONCLUSION

In this paper, an improved facial pore detection algorithm that combines the characteristics of skin pigment distribution and optimal scale was proposed. The experimental result shows its accuracy and efficiency on pore detection and interference filtering, and provides more reliable and detailed information for skin research, cosmetics development, face recognition, and other fields in the future.

## 5. REFERENCES


[1] Dong Li, Huiling Zhou, and Kin-Man Lam, "High-resolution face verification using pore-scale facial features," *IEEE transactions on image processing*, vol. 24, no. 8, pp. 2317–2327, 2015.

[2] J. Y. Sun, S. W. Kim, S. H. Lee, J. E. Choi, and S.J. Ko, "Automatic facial pore analysis system using multi-scale pore detection," *Skin Research and Technology*, vol. 23, no. 3, pp. 354–362, 2017.

[3] X. Wang, Y. Liang, X. Zeng, D. Li, and W. Jia, "Deeply learned pore-scale facial features," in *Chinese Conference on Biometric Recognition*, 2017, pp. 135–144.

[4] S. I. Jang, E. J. Kim, and H. K. Lee, "A method of evaluating facial pores using optical 2d images and analysis of agedependent changes in facial pores in koreans," *Skin Research and Technology*, vol. 24, no. 2, pp. 304–308, 2018.

[5] J. A. McGrath, R. A. J. Eady, and F. M. Pope, *Anatomy and Organization of Human Skin. Rooks textbook of dermatology*, Blackwell Publishing, 2004.

[6] S. Malathi and C. Meena, "Improved partial fingerprint matching based on score level fusion using pore and sift features," in *International Conference on Process Automation, Control and Computing*, 2011, pp. 1–4.

[7] D. G. Lowe, "Distinctive image features from scale-invariant keypoints," *International Journal of Computer Vision*, vol. 60, no. 2, pp. 91–110, 2004.

[8] D. Li and K. M. Lam, "Design and learn distinctive features from pore-scale facial keypoints," *Pattern Recognition*, vol. 48, no. 3, pp. 732–745, 2015.

[9] X. Zeng, Y. Zhang D. Li, and K. M. Lam, "Pore-scale facial features matching under 3d morphable model constraint," in *CCF Chinese Conference on Computer Vision*, 2017.

[10] N. Tsumura, H. Haneishi, and Y. Miyake, "Independent-component analysis of skin color image," *Journal of the Optical Society of America A Optics Image Science & Vision*, vol. 16, no. 9, pp. 2169–2176, 1999.

[11] C. Villegas, J. Climent, and C. Villegas, "Using skin melanin layer for facial pore identification in rgb digital images," *International Journal of Emerging Technology and Advanced Engineering*, vol. 4, no. 8, pp. 335–342, 2014.

[12] Z. Liu and J. Zerubia, "Melanin and hemoglobin identification for skin disease analysis," in *2nd IAPR Asian Conference on Pattern Recognition, IEEE*, 2013.

[13] R. Jolivot, Y. Benezeth, and F. Marzani, "Skin parameter map retrieval from a dedicated multispectral imaging system applied to dermatology/cosmetology," *Journal of Biomedical Imaging*, vol. 2013, no. 26, pp. 1–15, 2013.

[14] Yao Ning, Qing Zeng, Qing Wang, and Li Li, "Evaluating photographic scales of facial pores and diagnostic agreement of tests using latent class models," *Journal of Cosmetic & Laser Therapy*, vol. 19, no. 1, pp. 64–67, 2017.

[15] A Shaiek, F Flament, G Franois, V L. Descamps, C Barla, M Vicic, F Giron, and R Bazin, "A new tool to quantify the geometrical characteristics of facial skin pores. changes with age and a making-up procedure in caucasian women," *Skin research and technology*, vol. 23, no. 2, pp. 249–257, 2017.

[16] J. O. Joswig and T. Lorenz, "Detecting and quantifying geometric features in large series of cluster structures," *Zeitschrift fr Physikalische Chemie*, vol. 230, pp. 1057–1066, 2016.

[17] Herbert Bay, Andreas Ess, Tinne Tuytelaars, and Luc Van Gool, "Speeded-up robust features (surf)," *Computer Vision and Image Understanding*, vol. 110, no. 3, pp. 346–359, 2008.

[18] Takanori Igarashi, Ko Nishino, and Shree K. Nayar, "The appearance of human skin: a survey," *Foundations & Trends in Computer Graphics & Vision*, vol. 3, no. 1, pp. 1–95, 2007.

[19] M Hiraoka, M Firbank, M Essenpreis, M Cope, SR Arridge, P Van Der Zee, and DT Delpy, "A monte carlo investigation of optical pathlength in inhomogeneous tissue and its application to near-infrared spectroscopy," *Physics in Medicine & Biology*, vol. 38, no. 12, pp. 1859–1876, 1993.

[20] G. Francois, A. Maudet, and D. McDaniel, "Quantification of facial pores using image analysis," *COSMETIC DERMATOLOGY-CEDAR KNOLLS*, vol. 22, no. 9, pp. 457–465, 2009.

[21] Thanh N Tran, Klaudia Drab, and Michal Daszykowski, "Revised dbscan algorithm to cluster data with dense adjacent clusters," *Chemometrics and Intelligent Laboratory Systems*, vol. 120, pp. 92–96, 2013.

[22] Arman Savran, Neşe Alyüz, Hamdi Dibeklioğlu, Oya Çeliktutan, Berk Gökberk, Bülent Sankur, and Lale Akarun, "Bosphorus database for 3d face analysis," in *European Workshop on Biometrics and Identity Management*. Springer, 2008, pp. 47–56.